SIEMENS Healthineers

^{99m}Tc MDP SPECT/CT imaging in diagnosing Erdheim-Chester disease

By Xuezhong Chen, MD, Jianbo Yang, MD, and Qing Zhang, MD
Data and images courtesy of Nanchang University, Nanchang, China

History

A 47-year-old female presented with a two-year history of progressive exophthalmos. An MRI scan showed bilateral orbital masses in the retro-ocular space.

Resection surgery was performed for the left orbital mass. Histopathology showed scattered, nested foam-like tissue cells in the fibrous stroma with scattered focal mononuclear lymphocyte infiltration. Immune histochemistry showed the following: CD20 (+), CD3 (scattered +), CD43 (scattered +), CD5 (scattered +), CD68 (+), CD1a (-), S-100 (-), Ki-67 (low proliferation). No specific treatment was given following surgery.

The patient experienced dysphagia for two weeks. A head and body CT showed bilateral exophthalmos resulting from bilateral orbital soft-tissue masses. There were also bilateral perinephric, pericardial, and pelvic exudates (Figure 1).

The patient underwent ^{99m}Tc MDP bone imaging on a Symbia Intevo Bold™ SPECT/CT scanner for evaluation of whole-body skeletal metabolism.

The study was performed 3 hours following intravenous (IV) injection of 14.6 mCi of ^{99m}Tc MDP. Whole-body planar imaging followed by SPECT/CT with xSPECT Bone™ of the knees and conventional SPECT/CT tomography of the thorax was performed.

Findings

As noted in Figure 2, whole-body planar images show intense but symmetrical hypermetabolism at the proximal ends of the bilateral wrist joints, the long bones of the lower extremities, especially metaphyseal region of the bilateral distal femur and femoral condyles, as well as the proximal tibial shaft and tibial plateau. Focal areas of intense uptake were also visualized in the sternum, several thoracic vertebrae, and ribs.

In Figures 3 and 4, the SPECT/CT shows diffuse sclerosis in the shaft of the distal femur and proximal tibia, which corresponds to intense skeletal hypermetabolism correlating with the hypermetabolic zones defined on the planar images. Focal sclerotic lesions in the thoracic vertebrae, sternum, and ribs also reflect the diffuse nature of the disease process shown on planar images.

The pattern of skeletal involvement and the presence of bilateral orbital infiltration as well as perinephric and pericardial exudates together with histopathological confirmation from the retro-ocular left orbital mass excised (Figure 5) lead to a diagnosis of Erdheim-Chester disease (ECD).

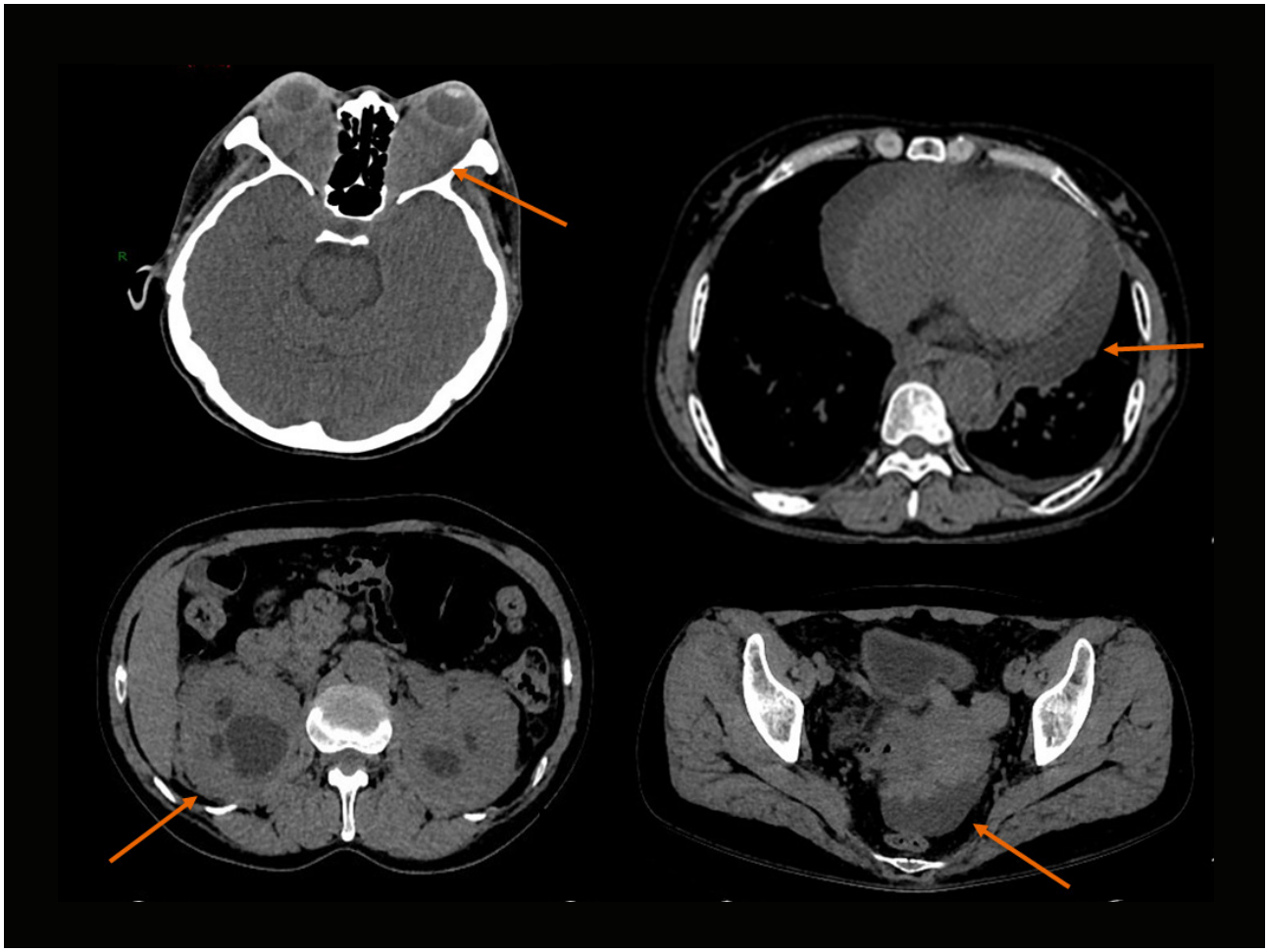

1 **CT shows bilateral orbital retro-ocular masses causing exophthalmos along with bilateral perinephric, pericardial, and pelvic exudates (arrows).**

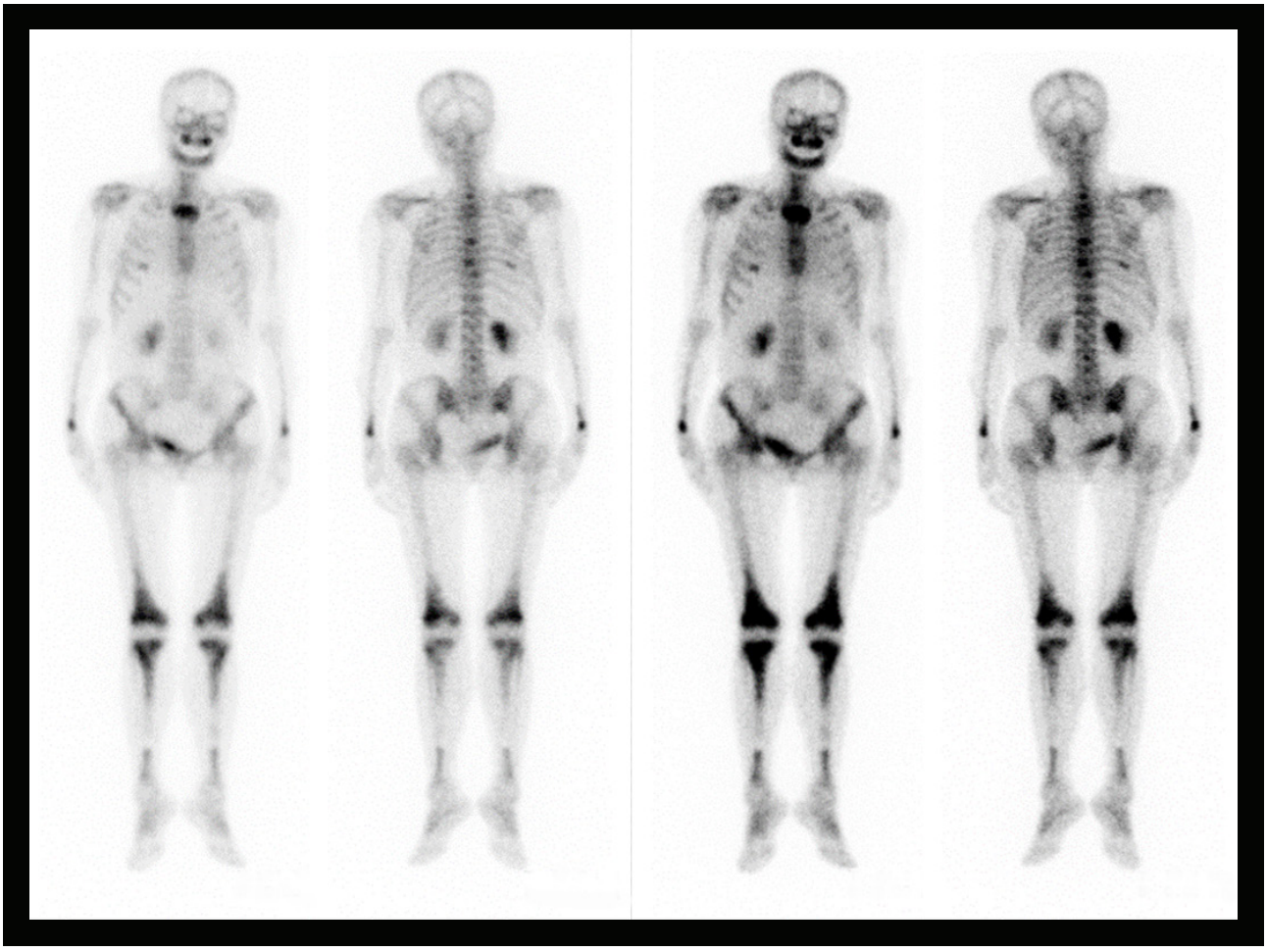

2 **Planar whole-body bone images show symmetrical hypermetabolism in the bilateral distal femur, proximal tibia, and distal ulna and radius.**

Discussion

ECD is a non-Langerhans-cell histiocytosis, originally defined as lipogranuloma lesions characterized by infiltration of tissues by foamy histerismos, multinucleated giant cells, and lipid-laden macrophages commonly associated with exophthalmos, symmetrical long-bone involvement, and extraskeletal involvement involving the kidneys, skin, and heart. In 2016, the World Health Organization reclassified this disease as histiocytic and dendritic cell tumors.[1] Due to the rarity of ECD and the diversity of clinical manifestations, diagnosis is extremely challenging. An ECD diagnosis depends on the histopathology of the biopsy specimen and immunohistochemistry results.[2] Radionuclide bone imaging, CT, MRI, and other imaging methods also have important diagnostic value in ECD. The standard diagnosis procedure should be based on the clinical and imaging studies to determine the biopsy site and further histopathological confirmation.

More than 95% of ECD patients have cortical sclerosis in the diaphysis and metaphysis of long bones with the distal femur, proximal tibia, and distal tibia being most typically involved.[3] Radionuclide bone imaging is highly sensitive to the presence of ECD-related changes in affected bones. ^{99m}Tc MDP SPECT/CT of the lesion can be used to observe the sclerosis of the shaft and metaphyses of long bones of the limbs. The whole-body planar bone images of this patient showed the typical characteristics of ECD, including symmetrical concentration of radionuclides in the shaft and metaphyses of the long bones of the lower extremities as well as the distal ulna and radius. Involvement of the shaft of the long bones is typically limited to the distal and proximal end of the shaft as seen in the bilateral distal femur, distal and proximal tibial shaft, and distal radius. Hypermetabolism and corresponding sclerosis were denser towards the metaphyseal end compared to rest of the shaft.

ECD is a rare disease and can be easily missed. In this case, symptoms such as exophthalmos, dizziness, and dysarthria occurred successively,

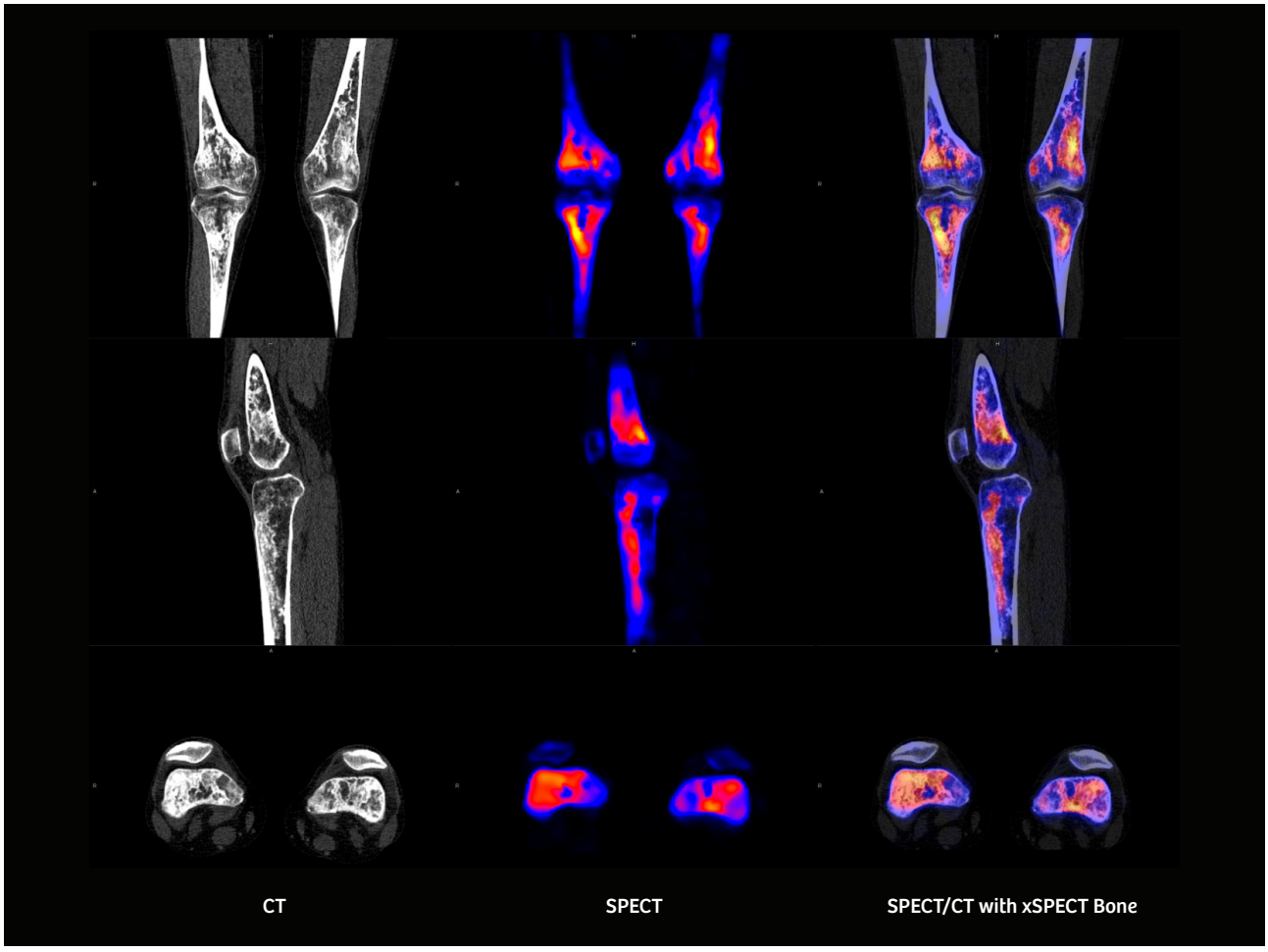

3 SPECT/CT with xSPECT Bone reconstruction of bilateral knees shows extensive scattered punctate sclerosis within the marrow of the lower femur and upper tibia, which corresponds to intense hypermetabolism sharply defined on xSPECT Bone. Zones of focal osteolysis are interspersed between sclerotic foci. No periosteal elevation or cartilage or joint space involvement was visualized.

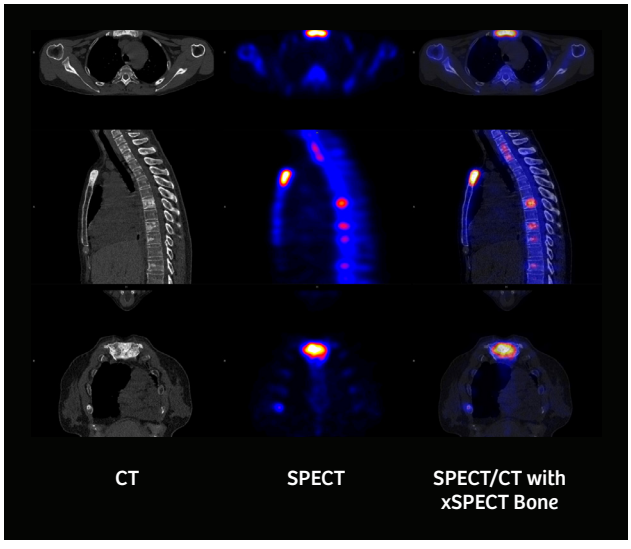

4 SPECT/CT of the thorax shows zones of sclerosis along with focal osteolysis within some thoracic vertebrae and the sternum as well as several ribs.

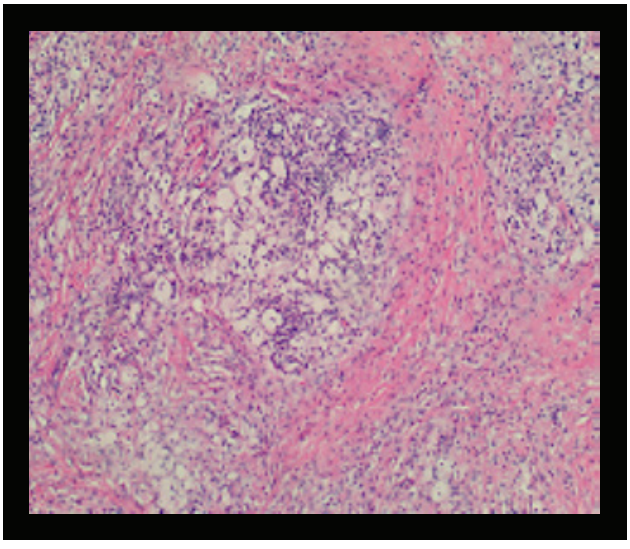

5 The histopathology result of tissue behind the left eyeball shows lipid granuloma lesions infiltrate, mainly composed of foam-like tissue cells and proliferating fibrous tissue (Hematoxylin and Eosin [H&E staining], magnification ×200).

but the diagnosis of ECD was not considered. Therefore, there is a need for pathologists, radiologists, and clinicians to increase their awareness of ECD and its manifestations. The patient reported here had predominant bone involvement along with the central nervous system, peripheral kidney, and retroperitoneum. Retroperitoneal and pelvic involvement in ECD is rare.

^{99m}Tc MDP SPECT/CT imaging has high diagnostic sensitivity for early skeletal involvement. Fusion imaging enables further evaluation of bone sclerosis and has important clinical value for the diagnosis of skeletal involvement in ECD patients. Symmetrical concentration of radionuclides and osteosclerosis in the long bones of the extremities is a typical imaging manifestation of ^{99m}Tc MDP SPECT/CT imaging of bone involvement in ECD patients.[4] When ^{99m}Tc MDP SPECT/CT imaging shows the long bones of the limbs are symmetrically concentrated with radionuclides and osteosclerosis, and other lesions involve corresponding symptoms, the possibility of ECD should be considered.

Conclusion

^{99m}Tc MDP SPECT/CT imaging with xSPECT Bone is an economical and simple method in diagnosing ECD, and may help provide early diagnosis, guide biopsy, and evaluate treatment response.[5] ●

Examination protocol

Scanner: Symbia Intevo Bold

SPECT		CT	
Injected dose	14.6 mCi (540.2 MBq) ^{99m}Tc MDP	Tube voltage	130 kV
Post-injection delay	3 hours	Tube current	41 mAs
Acquisition	**Planar imaging** Scan speed: 25 cm/min Matrix: 256 x 1024, Zoom 1.0 **SPECT tomography** Scan speed: 25 s/stop, 32 stops/detector, Matrix: 256 x 256, Zoom 1.0 **xSPECT Bone** Scan speed: 18 s/stop, 60 stops/detector, Matrix: 256 x 256, Zoom 1.0	Slice collimation	0.6 mm
Scan time	• Planar imaging: 8 min • SPECT tomography: 15 min • xSPECT Bone: 22 min	Slice thickness	.75 mm
		Reconstruction kernel	B60s

The outcomes achieved by the Siemens Healthineers customers described herein were achieved in the customer's unique setting. Since there is no "typical" hospital and many variables exist (eg, hospital size, case mix, level of IT adoption) there can be no guarantee that others will achieve the same results.

References

1 Swerdlow SH, Campo E, Pileri SA, et al. The 2016 revision of the World Health Organization classification of lymphoid neoplasms. *Blood.* 2016;127(20):2375-90. doi:10.1182/blood-2016-01-643569.

2 Haroche J, Amoura Z, Wechsler B, Veyssier-Belot C, Charlotte V, Piette JC. Erdheim-Chester disease. *Presse Med.* 2007;36(11 Pt 2):1663-8. doi:10.1016/j.lpm.2007.04.032

3 Mamlouk MD, Aboian MS, Glastonbury CM. Case 245: Erdheim-Chester Disease. *Radiology.* 2017;284(3):910-17. doi:10.1148/radiol.2017141151.

4 Tsai JW, Tsou JH, Hung LY, et al. Combined Erdheim-Chester disease and Langerhans cell histiocytosis of skin are both monoclonal: a rare case with human androgen-receptor gene analysis. *J Am Acad Dermatol.* 2010;63(2):284-91. doi:10.1016/j.jaad.2009.08.013.

5 Goyal G, Shah MV, Call TG, et al. Clinical and Radiologic Responses to Cladribine for the Treatment of Erdheim-Chester Disease. *JAMA Oncol.* 2017;3(9):1253-56. doi:10.1001/jamaoncol.2017.0041.

Siemens Healthineers Headquarters
Siemens Healthcare GmbH
Henkestr. 127
91052 Erlangen
Germany
Phone: +49 9131 84-0
siemens-healthineers.com

Published by
Siemens Medical Solutions USA, Inc.
2501 N. Barrington Road
Hoffman Estates, IL 60192-2061
USA
Phone: +1 847-304-7700
siemens-healthineers.com/mi

MI-5101.BM.JV · PDF only · © Siemens Healthcare GmbH, 03.2021

siemens-healthineers.com/micc